In silico identification of lipid-binding α helices of uncoupling protein 1

YING JING*, YAHAN NIU*, CHANG LIU*, KE ZEN and DONGHAI LI

State Key Laboratory of Pharmaceutical Biotechnology, Jiangsu Engineering Research Center for MicroRNA Biology and Biotechnology, Nanjing Advanced Institute for Life Sciences (NAILS), School of Life Sciences, Nanjing University, Nanjing, Jiangsu 210023, P.R. China

Received April 15, 2018; Accepted July 19, 2018

DOI: 10.3892/br.2018.1133

Abstract. Uncoupling protein 1 (UCP1) located at the mitochondrial inner membrane serves an important role in adaptive non-shivering thermogenesis. Previous data has demonstrated that membrane lipids regulate the biological functions of membrane proteins. However, how mitochondrial lipids interact with UCP1 still remains elusive. In this study, the interactions between UCP1 and membrane lipids were investigated, using bioinformatic approaches due to the limitations associated with experimental techniques. A total of 8 UCP1 peptide regions with α-helices were identified and related to functional sites of UCP1. These were all novel peptide sequences compared with the known protein-lipid interactions. Among several types of UCP1-binding molecules, cardiolipin appeared to serve as a key interacting molecule of the 8 lipid-binding α-helix regions of UCP1. Two cardiolipin-binding lysines (K^{175} and K^{269}) of UCP1 may be crucial for this UCP1-cardiolipin recognition and UCP1 function. The present findings provide novel insight into the associations of UCP1 with lipids and the potential drug targets in UCP1-associated diseases.

Introduction

Mitochondrial uncoupling protein 1 (UCP1), which is expressed in brown adipose tissue (BAT), is a critical regulator of adaptive non-shivering thermogenesis via the biological function of proton leak (1-4). UCP1, a transmembrane protein, is located at the inner mitochondrial inner membrane, and uncouples the oxidative phosphorylation to produce heat through decreasing the proton gradients (1,2). Free fatty acids are the established activators that reduce the transmembrane potential via UCP1 and increase UCP1-associated oxygen consumptions (5). Chouchani *et al* (6) identified the sulfenylation of UCP1 regulated by mitochondrial reactive oxygen species in 2016. Uncoupling proteins (UCPs) expressed in adipose cells, skeletal muscle and macrophages participate in fatty acid metabolism (7,8). In addition, UCPs have been associated with metabolic diseases, including obesity and diabetes (9,10).

Subcellular compartments from yeast to mammalian cells contain numerous proteins and lipids. Phosphatidylcholine and phosphatidylethanolamine are major mitochondrial phospholipids (~80%). High cardiolipin content (10-15%) is found in mitochondrial membranes and its concentration is implicated in human health and disease (11,12). Protein-lipid interactions are crucial for protein stability (12). Cardiolipin directly interacts with ADP/ATP translocase (ANT) at the mitochondrial inner membrane (13), and *in vitro* reconstituted experiments have demonstrated the binding of six molecules of cardiolipin per ANT dimer (14). The exact associations of UCP1 with mitochondrial inner membrane lipids still remain unknown. In the present study, bioinformatics was used to identify the lipid-binding α-helix regions of UCP1. The results may provide novel insight into UCP1-lipid binding.

Materials and methods

Prediction of lipid-binding α-helices of UCP1. Mouse UCP1 protein sequence (P12242) was obtained from the UNIPROT database (http://www.uniprot.org/) (15). The HeliQuest web server (http://heliquest.ipmc.cnrs.fr/) was used to predict the lipid-binding α-helices of UCP1 through calculations of mean hydrophobicity, hydrophobic moment and net charge (16). These scores were further analyzed in order to calculate the discrimination factor, which was considered to filter the possible/confident lipid-binding α-helices according to HeliQuest instructions. The Basic Local Alignment Search Tool (BLAST; https://blast.ncbi.nlm.nih.gov/) was used to determine sequence identity.

Correspondence to: Dr Donghai Li, State Key Laboratory of Pharmaceutical Biotechnology, Jiangsu Engineering Research Center for MicroRNA Biology and Biotechnology, Nanjing Advanced Institute for Life Sciences (NAILS), School of Life Sciences, Nanjing University, Nanjing, Jiangsu 210023, P.R. China
E-mail: donghaili@nju.edu.cn

*Contributed equally

Abbreviations: ANT, ADP/ATP translocase; BAT, brown adipose tissue; DOPE, discrete optimized protein energy; UCP1, uncoupling protein 1; UCPs, uncoupling proteins; 3D, three-dimensional

Key words: adaptive non-shivering thermogenesis, cardiolipin, protein-lipid interaction, uncoupling protein 1

Helical wheel plots. Helical wheel plots are commonly used to represent amphiphilic helices. In the present analysis, the helical wheel diagrams were drawn using the Wenxiang server (http://www.jci-bioinfo.cn/wenxiang2) (17).

Template selection. Template selection for the target protein (UCP1) was performed in SWISS-MODEL (http://swiss-model.expasy.org/workspace/) and MODELLER v9.16 (https://salilab.org/modeller/) (18,19). InterPro Domain Scan (HMMPfam, HMMTigr, ProfileScan, SuperFamily and BlastProDom), Gapped Blast Query and HHSearch template library search in SWISS-MODEL were used to search for templates. Structural resolutions were also considered.

Homology model building. Primary sequences of templates and target protein were obtained from the UNIPROT database and template PDB files using MODELLER script. Template-target sequence alignment was also completed by MODELLER script with the consideration of SWISS-MODEL results. A three-dimensional (3D) homology model of UCP1 was built using MODELLER v9.16.

Energy minimization and model evaluation. The UCP1 homology model generated by MODELLER v9.16 was ranked and scored using the discrete optimized protein energy (DOPE) score. The best homolog model of UCP1 was evaluated with PROCHECK (https://www.ebi.ac.uk/thornton-srv/software/PROCHECK/) (20). The final structure was visualized in PyMOL 1.7.0.0 (https://pymol.org) (21).

UCP1-lipid docking model. Similar to the homology model building, the docking model of UCP1 and lipids was generated in MODELLER v9.16. The same templates were analyzed to predict the docking model. The best docking model was selected according to the DOPE score. The main docking molecules contained B-nonylglucoside and cardiolipin.

Protein-lipid interaction analysis. The detailed interactions of UCP1 and lipids were displayed in PyMOL 1.7.0.0 and analyzed with LigPlot$^+$ 1.4 (https://www.ebi.ac.uk/thornton-srv/software/LigPlus/) (22). LigPlot$^+$ draws a two-dimensional diagram of ligand-protein interactions from 3D coordinates, which shows the hydrogen-bond interaction patterns and hydrophobic contacts between the ligands and proteins.

Results and Discussion

Mitochondrial UCP1 is specifically expressed in mammalian BAT. Thus far, to our knowledge, its high-resolution structure has not been determined. Reportedly, UCP1 as a mitochondrial transmembrane protein interacts with mitochondrial lipids, which considerably affects its biological function (23). In the current study, the putative lipid-binding α-helices of UCP1 were determined by bioinformatics. The HeliQuest algorithm has successfully predicted the lipid-binding sites of membrane proteins previously (16). The overall HeliQuest-calculated scores (mean hydrophobicity, hydrophobic moment and net charges) are presented in Fig. 1A. Following further discrimination factor-based analyses, a total of 8 lipid-binding α-helix regions of UCP1 were identified (^{37}AKVRLQIQGEGQASSTIR^{54}, ^{56}KGVLGTITTLAKTEGLPK^{73}, ^{75}YSGLPAGIQRQISFASLR^{92}, ^{134}TEVVKVRMQAQSHLHGIK^{151}, ^{166}TTESLSTLWKGTTPNLMR^{183}, ^{235}VVKTRFINSLPGQYPSVP^{252}, ^{260}TKEGPTAFFKGFVASFLR^{277} and ^{283}VIMFVCFEQLKKELMKSR^{300}). These predicted results may be considered acceptable among the range of strategies available to calculate the discrimination factor. The helical wheel plots of lipid-binding α-helix regions of UCP1 are shown in Fig. 1B. Helical wheel plots with an 18 amino acid window are considered to depict the best α-helices (16). As shown in Fig. 1B, the identified lipid-binding α-helix regions displayed the amphiphilic properties. The amino acid sequences of the lipid-binding α-helix regions of UCP1 exhibited no high sequence identities with other known lipid-binding domains (C1, C2, PH, FYVE, PX, ENTH, ANTH, BAR, FERM, PDZ or tubby domains), indicating that these lipid-binding regions were the novel lipid-binding sites. Of these lipid-binding regions of UCP1, the fourth region (^{134}TEVVKVRMQAQSHLHGIK^{151}) was a highly confident lipid-binding peptide based on the subsequent screening scores of HeliQuest. The peptide with 100% sequence identity was indicated to be exclusively found in mice and rats by BLAST, and may be a crucial interacting sequence for UCP1-lipid associations and UCP1 stability. Furthermore, there were some sequence similarities among these novel lipid-binding α-helix regions despite the lack of peptides with 100% sequence identity. For example, the above-mentioned fourth lipid-binding protein region had a 47% sequence similarity to ^{14}NDRTLRRMRKVVNIINAME^{33} (*Escherichia coli* SecA) as predicted by HeliQuest (24).

To assess the 3D structure of UCP1, acceptable templates were searched for with high sequence identity. Their sequence alignment is presented in Fig. 2A. Functional BAT and UCP1 have been identified and characterized in rodents and human (25,26). *In silico* analysis of mouse UCP1 is performed since rodents generally work as important validated targets prior to clinical trials, and BAT with UCP1 expression is easily identifiable in small mammals including mice (26,27). The crystal structures of *Bos taurus* and *Saccharomyces cerevisiae* ANT carriers (PDB IDs: 2c3e and 4c9g) (28,29) were used to build a final homology model of UCP1. An available NMR structure of UCP2 with high sequence identity to UCP1 was not selected due to its low resolution (30). The PROCHECK program was used to evaluate the reliability and reasonability of the model, with >95% residues in most-favored/additionally allowed/generously allowed regions. Surprisingly, the 8 lipid-binding α-helix regions were mostly present outside the six main helix bundles of UCP1 (Fig. 2B), suggesting that the interactions of lipid-binding α-helices belonged to nonannular protein-lipid interactions (31). Previous observations have demonstrated that mutations of certain residues significantly influence the biological function of UCP1 (9). Of these sites, P^{79}, R^{84}, R^{92}, E^{135}, M^{141}, H^{146}, H^{148}, E^{168}, R^{183}, ^{262}EGPTAFFKG^{270} and R^{277} are located at the lipid-binding α-helix regions (9), and these sites associated with the lipid-binding α-helix regions may involve the biological function of UCP1. It is hypothesized that mutations alter protein functions via the conformational disturbances theoretically caused by the physicochemical properties of amino acid residues (32-34). Another possible complementary explanation is that these mutations of membrane proteins may disturb the

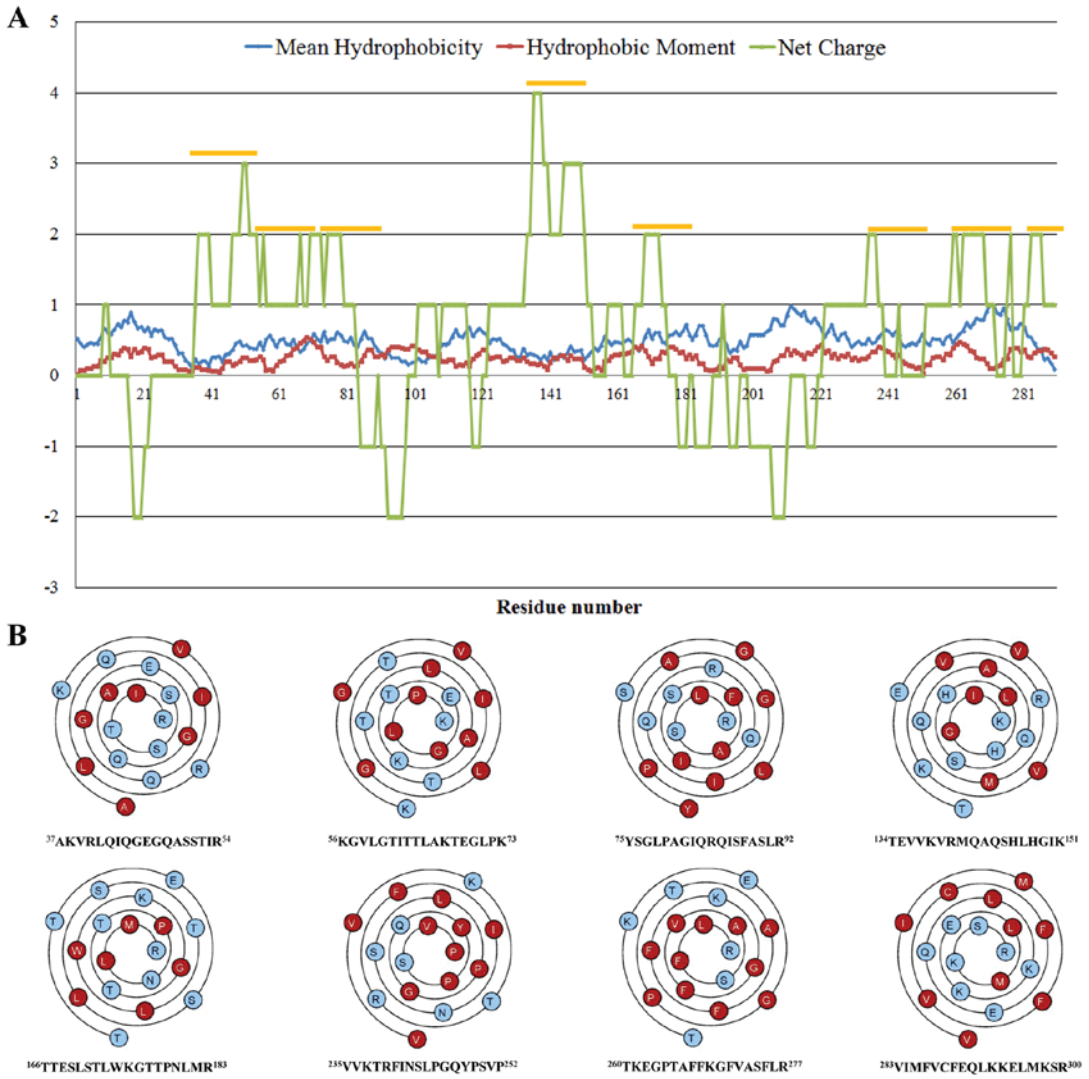

Figure 1. Mean hydrophobicity, hydrophobic moment, net charge and helical wheel plots of the lipid-binding regions of UCP1. (A) Mean hydrophobicity, hydrophobic moment and net charge calculated by HeliQuest. (B) Helical wheel diagrams. The orange bars represent the lipid-binding α-helix regions of UCP1. The red-filled circles and blue-filled circles represent hydrophobic and hydrophilic residues, respectively. UCP1, uncoupling protein 1.

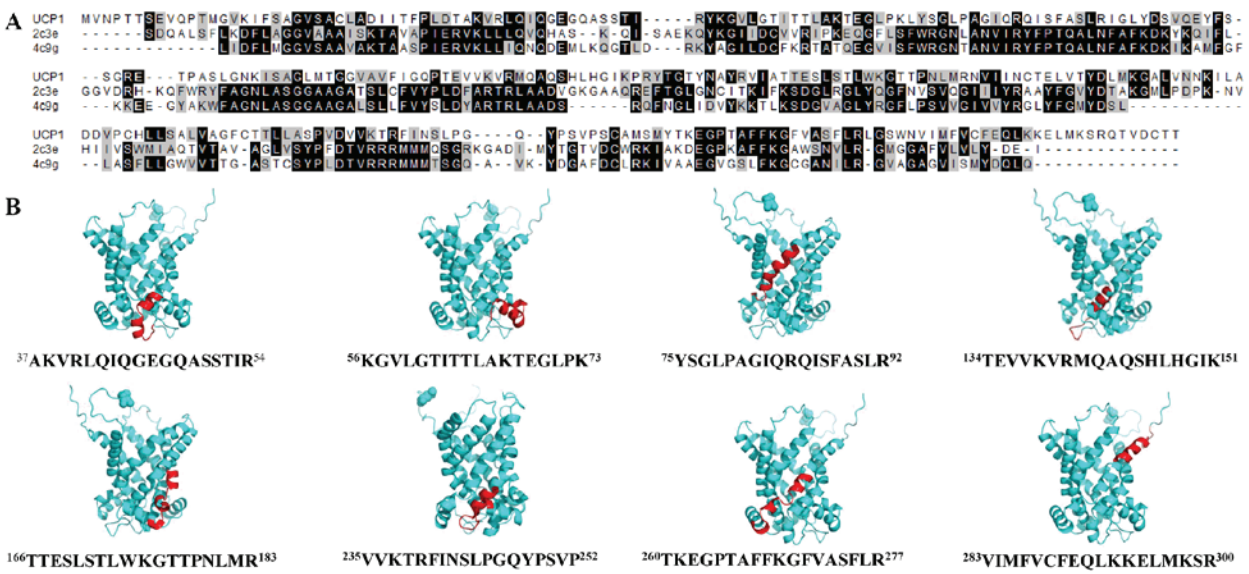

Figure 2. Sequence alignment and locations of the lipid-binding regions of UCP1. (A) Sequence alignment of UCP1 and its templates (sc3e and 4c9g). (B) Location of lipid-binding α-helix regions (red) in the UCP1 homology model. The N-terminal amino acid residue of UCP1 is shown in spheres. UCP1, uncoupling protein 1.

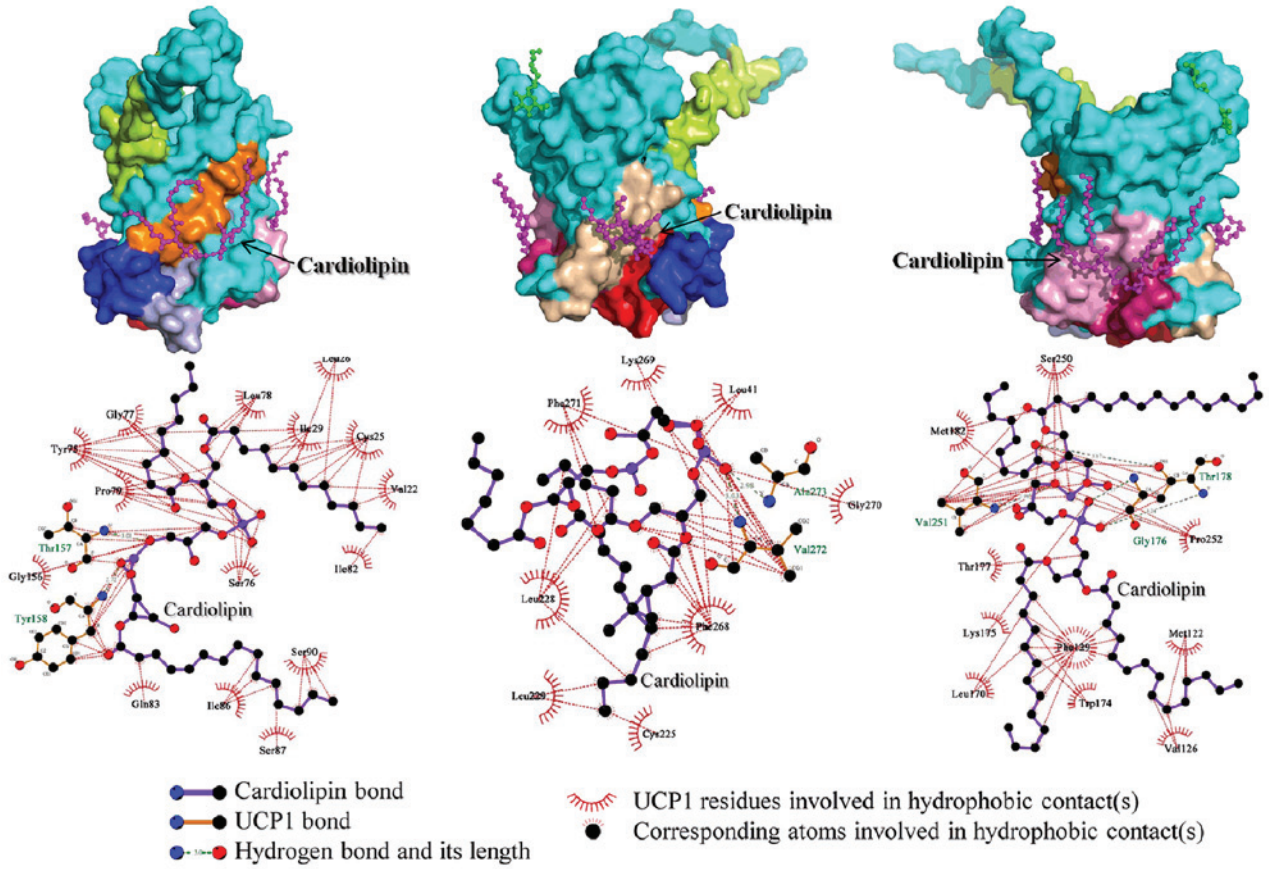

Figure 3. Interactions between UCP1 and lipids. The detailed interactions of UCP1 and three cardiolipins analyzed by LigPlot+ are shown, and the relevant peptides/molecules are highlighted: ^{37}AKVRLQIQGEGQASSTIR^{54} (red), ^{56}KGVLGTITTLAKTEGLPK^{73} (blue), ^{75}YSGLPAGIQRQISFASLR^{92} (orange), ^{34}TEVVKVRMQAQSHLHGIK^{151} (light blue), ^{166}TTESLSTLWKGTTPNLMR^{183} (pink), ^{35}VVKTRFINSLPGQYPSVP^{252} (warm pink), ^{260}TKEGPTAFFKGFVASFLR^{277} (wheat), ^{83}VIMFVCFEQLKKELMKSR^{300} (lemon), B-nonylglucoside (green) and cardiolipin (magenta). UCP1, uncoupling protein 1.

protein-lipid interactions, thus causing the protein instability or conformational abnormalities.

Cardiolipin acts as an insulator and stabilizes mitochondrial membrane proteins, including mitochondrial respirasome (35). As shown in Fig. 3, the putative lipid-binding α-helix regions of UCP1 in the current UCP1-lipid docking model appeared to mainly associate with three cardiolipins; an interaction eluded to previously (23). LigPlot+ analysis demonstrated a variety of hydrophobic and hydrophilic interactions between UCP1 and cardiolipins (Fig. 3B); indeed cardiolipin might be a key regulator of optimal biological activity of many membrane proteins (36). An example is cardiolipin-binding cytochrome c oxidase. Of these cardiolipin-related interactions determined by LigPlot+, the main interacting contributors of UCP1 appeared to be ^{75}YSGLPAGIQRQISFASLR^{92}, ^{166}TTESLSTLWKGTTPNLMR^{183}, ^{235}VVKTRFINSLPGQYP SVP^{252} and ^{260}TKEGPTAFFKGFVASFLR^{277}. The lysine residues of cardiolipin-binding cytochrome c seem to be crucial for their recognition and biological activities (37). In the current docking model, two lysines (K^{175} and K^{269}) were revealed to bind to cardiolipins. The interactions may be implicated in the same function related to the cytochrome c-cardiolipin complex. However, the exploration of these interactions between UCP1 and cardiolipins still requires high-resolution or standard biophysical techniques. Previous studies have demonstrated that cardiolipin may be a potential target for therapies against Parkinson's disease; the current results indicate that it may be a promising therapeutic target in UCP1-associated diseases.

Protein-lipid interactions contribute to the structural stability and biological function of transmembrane proteins. We herein analyzed the lipid-binding α-helix regions of mitochondrial UCP1, using bioinformatic approaches due to the limitations of experimental techniques in this field. A total of 8 plausible lipid-binding α-helix regions of UCP1 were predicted based on the characteristics of protein-lipid interactions. These interaction regions also mapped onto the key functional regions of UCP1, suggesting that these lipid-binding regions are involved in the biological function of UCP1. The UCP1-lipid docking model indicate that cardiolipin is a crucial interacting molecule and may maintain optimal biological function. The findings support the presence of specific lipid-binding α-helices in UCP1 that may represent the therapeutic targets for UCP1-associated diseases.

Acknowledgements

Not applicable.

Funding

The present study was supported by the National Natural Science Foundation of China (grant nos. 31470716, 31000323,

31070672 and 31770981) and the Natural Science Foundation of Jiangsu Province (grant no. BK20131272).

Availability of data and materials

The datasets used and/or analyzed during the current study are available from the corresponding author on reasonable request.

Authors' contributions

YJ, YN, CL and KZ performed the experiments and analyzed the data. DL designed and performed the experiments, analyzed data, and drafted the manuscript. All authors approved the final version to be published.

Ethics approval and consent to participate

Not applicable.

Consent for publication

Not applicable.

Competing interests

The authors declare that they have no competing interests.

References

1. Bertholet AM and Kirichok Y: UCP1: A transporter for H^+ and fatty acid anions. Biochimie 134: 28-34, 2017.
2. Bonet ML, Mercader J and Palou A: A nutritional perspective on UCP1-dependent thermogenesis. Biochimie 134: 99-117, 2017.
3. Crichton PG, Lee Y and Kunji ERS: The molecular features of uncoupling protein 1 support a conventional mitochondrial carrier-like mechanism. Biochimie 134: 35-50, 2017.
4. Marlatt KL and Ravussin E: Brown adipose tissue: an update on recent findings. Curr Obes Rep 6: 389-396, 2017.
5. Fedorenko A, Lishko PV and Kirichok Y: Mechanism of fatty-acid-dependent UCP1 uncoupling in brown fat mitochondria. Cell 151: 400-413, 2012.
6. Chouchani ET, Kazak L, Jedrychowski MP, Lu GZ, Erickson BK, Szpyt J, Pierce KA, Laznik-Bogoslavski D, Vetrivelan R, Clish CB, *et al*: Mitochondrial ROS regulate thermogenic energy expenditure and sulfenylation of UCP1. Nature 532: 112-116, 2016.
7. Rousset S, Alves-Guerra MC, Mozo J, Miroux B, Cassard-Doulcier AM, Bouillaud F and Ricquier D: The biology of mitochondrial uncoupling proteins. Diabetes 53: S130-S135, 2004.
8. Kopecky J, Rossmeisl M, Flachs P, Bardova K and Brauner P: Mitochondrial uncoupling and lipid metabolism in adipocytes. Biochem Soc T 29: 791-797, 2001.
9. Klingenspor M, Fromme T, Hughes DA Jr, Manzke L, Polymeropoulos E, Riemann T, Trzcionka M, Hirschberg V and Jastroch M: An ancient look at UCP1. Biochim Biophys Acta-Bioenergetics 1777: S24-S24, 2008.
10. Sreedhar A and Zhao YF: Uncoupling protein 2 and metabolic diseases. Mitochondrion 34: 135-140, 2017.
11. Zinser E and Daum G: Isolation and biochemical characterization of organelles from the Yeast, Saccharomyces cerevisiae. Yeast 11: 493-536, 1995.
12. Horvath SE and Daum G: Lipids of mitochondria. Prog Lipid Res 52: 590-614, 2013.
13. Lawson JE, Gawaz M, Klingenberg M and Douglas MG: Structure-function studies of adenine nucleotide transport in mitochondria. I. Construction and genetic analysis of yeast mutants encoding the ADP/ATP carrier protein of mitochondria. J Biol Chem 265: 14195-14201, 1990.
14. Claypool SM: Cardiolipin, a critical determinant of mitochondrial carrier protein assembly and function. Biochim Biophys Acta 1788: 2059-2068, 2009.
15. The UniProt C: UniProt: the universal protein knowledgebase. Nucleic Acids Res 45: D158-D169, 2017.
16. Gautier R, Douguet D, Antonny B and Drin G: HELIQUEST: a web server to screen sequences with specific α-helical properties. Bioinformatics 24: 2101-2102, 2008.
17. Chou KC, Lin WZ and Xiao X: Wenxiang: a web-server for drawing wenxiang diagrams. Nat Sci 3: 862-865, 2011.
18. Biasini M, Bienert S, Waterhouse A, Arnold K, Studer G, Schmidt T, Kiefer F, Gallo Cassarino T, Bertoni M, Bordoli L, *et al*: SWISS-MODEL: modelling protein tertiary and quaternary structure using evolutionary information. Nucleic Acids Res 42: W252-W258, 2014.
19. Webb B and Sali A: Protein structure modeling with MODELLER. Methods Mol Biol 1654: 39-54, 2017.
20. Laskowski RA, Rullmannn JA, MacArthur MW, Kaptein R and Thornton JM: AQUA and PROCHECK-NMR: programs for checking the quality of protein structures solved by NMR. J Biomol NMR 8: 477-486, 1996.
21. Yuan S, Chan HCS, Filipek S and Vogel H: PyMOL and Inkscape bridge the data and the data visualization. Structure 24: 2041-2042, 2016.
22. Laskowski RA and Swindells MB: LigPlot+: multiple ligand-protein interaction diagrams for drug discovery. J Chem Inf Model 51: 2778-2786, 2011.
23. Lee Y, Willers C, Kunji ERS and Crichton PG: Uncoupling protein 1 binds one nucleotide per monomer and is stabilized by tightly bound cardiolipin. Proc Natl Acad Sci USA 112: 6973-6978, 2015.
24. Keller RC: The prediction of novel multiple lipid-binding regions in protein translocation motor proteins: A possible general feature. Cell Mol Biol Lett 16: 40-54, 2011.
25. Cypess AM, Lehman S, Williams G, Tal I, Rodman D, Goldfine AB, Kuo FC, Palmer EL, Tseng YH, Doria A, *et al*: Identification and importance of brown adipose tissue in adult humans. N Engl J Med 360: 1509-1517, 2009.
26. Lau AZ, Chen AP, Gu Y, Ladouceur-Wodzak M, Nayak KS and Cunningham CH: Noninvasive identification and assessment of functional brown adipose tissue in rodents using hyperpolarized 13C imaging. Int J Obes (Lond) 38: 126-131, 2014.
27. Ong FJ, Ahmed BA, Oreskovich SM, Blondin DP, Haq T, Konyer NB, Noseworthy MD, Haman F, Carpentier AC, Morrison KM, *et al*: Recent advances in the detection of brown adipose tissue in adult humans: a review. Clin Sci (Lond) 132: 1039-1054, 2018.
28. Nury H, Dahout-Gonzalez C, Trezeguet V, Lauquin G, Brandolin G and Pebay-Peyroula E: Structural basis for lipid-mediated interactions between mitochondrial ADP/ATP carrier monomers. FEBS Lett 579: 6031-6036, 2005.
29. Ruprecht JJ, Hellawell AM, Harding M, Crichton PG, McCoy AJ and Kunji ER: Structures of yeast mitochondrial ADP/ATP carriers support a domain-based alternating-access transport mechanism. Proc Natl Acad Sci USA 111: E426-E434, 2014.
30. Berardi MJ, Shih WM, Harrison SC and Chou JJ: Mitochondrial uncoupling protein 2 structure determined by NMR molecular fragment searching. Nature 476: 109-113, 2011.
31. Contreras FX, Ernst AM, Wieland F and Brugger B: Specificity of intramembrane protein-lipid interactions. Cold Spring Harb Perspect Biol 3: a004705, 2011.
32. Gromiha MM, Oobatake M, Kono H, Uedaira H and Sarai A: Relationship between amino acid properties and protein stability: buried mutations. J Protein Chem 18: 565-578, 1999.
33. Gromiha MM, Oobatake M, Kono H, Uedaira H and Sarai A: Role of structural and sequence information in the prediction of protein stability changes: comparison between buried and partially buried mutations. Protein Eng 12: 549-555, 1999.
34. Gromiha MM, Oobatake M and Sarai A: Important amino acid properties for enhanced thermostability from mesophilic to thermophilic proteins. Biophys Chem 82: 51-67, 1999.
35. Guo R, Zong S, Wu M, Gu J and Yang M: Architecture of human mitochondrial respiratory megacomplex I2III2IV2. Cell 170: 1247-1257, 2017.
36. Planas-Iglesias J, Dwarakanath H, Mohammadyani D, Yanamala N, Kagan VE and Klein-Seetharaman J: Cardiolipin interactions with proteins. Biophys J 109: 1282-1294, 2015.
37. Sinibaldi F, Howes BD, Droghetti E, Polticelli F, Piro MC, Di Pierro D, Fiorucci L, Coletta M, Smulevich G and Santucci R: Role of lysines in cytochrome c-cardiolipin interaction. Biochemistry 52: 4578-4588, 2013.